

Fast Risk Assessment in Power Grids through Novel Gaussian Process and Active Learning

Parikshit Pareek, Deepjyoti Deka, and Sidhant Misra

Abstract—This paper presents a graph-structured Gaussian process (GP) model for data-driven risk assessment of critical voltage constraints. The proposed GP is based on a novel kernel, named the vertex-degree kernel (VDK), that decomposes the voltage-load relationship based on the network graph. To estimate the GP efficiently, we propose a novel active learning scheme that leverages the additive structure of VDK. Further, we prove a probabilistic bound on the error in risk estimation using VDK-GP model that demonstrates that it is statistically comparable to using standard AC power flow (AC-PF), but does not require computing a large number of ACPF solutions. Simulations demonstrate that the proposed VDK-GP achieves more than two fold sample complexity reduction, compared to a generic GP on medium scale 500-Bus and large scale 1354-Bus power systems. Moreover, active learning achieves an impressive reduction of over 15 times in comparison to the time complexity of Monte-Carlo simulations (MCS), and have risk estimation error of order 10^{-4} for both 500-Bus and 1354-Bus system, demonstrating its superior efficiency in risk estimation.

Index Terms—Physics-informed Learning, Additive Kernel, Power Flow Twin, Gaussian Process, Active Learning.

I. INTRODUCTION

Increase in uncertain power sources and variable loads means that ensuring secure power system operation has become more challenging than before [1]. An important problem in this context is voltage risk assessment (VRA) that aims to quantify the likelihood of a bus voltage exceeding its operational limit due to uncertainty [2]. The problem of VRA can also be viewed as uncertainty quantification (UQ) [3] for the distribution of output voltage under uncertain load for a given operating condition. Computationally, performing VRA is a challenge as Alternating Current Power Flow (ACPF) equations are nonlinear and are not expressed as analytical (or closed-form) expressions of nodal voltages with bus load vector as input [4], [5]. Instead, iterative methods such as the Newton-Raphson load flow (NRLF) must be employed, and can lead to significant computational overhead since accurate VRA requires a large number of power flow samples. On the other hand, the direct current approximation for PF [6], [7] neglects the voltage information, and therefore cannot be utilized to estimate voltage risk.

Recently, machine learning (ML) methods, in particular Deep Neural Networks (DNNs), have made significant advancements as universal function approximators, especially

in conjunction with the idea of physics-informed ML [8], [9]. They have also been explored for PF learning and UQ [10]–[12]. The idea behind learning ACPF is that a fast PF solver can be used as an *Oracle* to provide large number of voltage solutions for risk assessment [10]. However, DNNs require extremely large number of samples to learn the PF approximator. For instance, more than 10,000 training samples are used to learn voltage solutions for the 118-Bus system in [10]–[12]. Another limitation is that ML methods, in general, do not provide confidence bounds on their prediction. Such bounds are necessary for reliable constraint enforcement but requires a large number of NRLF solutions for out-of-sample validation.

In this work, we take an alternate modeling approach using Gaussian process (GP) for modeling voltage-injection characteristic and use it for VRA. Gaussian process (GP) learning [13] is a versatile probabilistic method for function estimation that enables flexible representation of uncertainty [13]. It has been applied to various power system applications [5], [14]–[18]. One notable drawback, common to all these GP works, is that their applicability has been restricted to small to medium-sized systems. This scale limitation is because exact GP inference has cubic complexity with respect to number of samples [13], which grows with system size (or input dimension). Moreover, previous DNN and standard GP models in grid applications do not provide any criteria to apriori decide the number of required training samples. The ability to assess the training quality ‘on the go’ and having a stopping criteria, is of great importance when risk-assessment needs to be done within a short amount of time.

In this paper, we propose to use a Vertex-Degree Kernel (VDK) based GP model for risk assessment of voltage, given an operating condition and load uncertainty set. VDK learns the *voltage-load* function in large-scale systems efficiently by breaking the Kernel function into additive lower-dimensional latent functions based on neighborhoods in the network topology. Further, the VDK-GP model is amenable for Active Learning (AL), an approach to reduce the overall sample complexity of training [19], where successive training point containing the *maximum information* about the unknown target function are selected [20]. AL for standard GP [5] suffers from *curse-of-dimensionality* as the search space grows exponentially with the dimension of input, which is the number of loads. We leverage the additive additive low-dimensional functions inside VDK-GP’s kernel for a novel network-swipe active learning (AL) algorithm to bypass the curse of dimensionality to further improve its efficiency.

Finally, we establish probabilistic error bounds on expected value estimation with generic ML models, that applies to probabilistic risk estimation using VDK-GP. We show that VDK-GP’s voltage outputs provides a fast alternative to solv-

Authors are with Theoretical Division (T-5), Los Alamos National Laboratory, NM, USA. Email: pareek,deepjyoti,sidhant@lanl.gov.

The authors acknowledge the funding provided by LANL’s Directed Research and Development (LDRD) project: “High-Performance Artificial Intelligence” (20230771DI) and The Department of Energy (DOE), USA under the Advanced grid Modeling (AGM) program. The research work conducted at Los Alamos National Laboratory is done under the auspices of the National Nuclear Security Administration of the U.S. Department of Energy under Contract No. 89233218CNA000001

ing standard AC-PF for computing the probability of voltage violations, while its theoretical error bound eliminates the need for any out-of-sample validation. In summary, the main contributions of this study can be delineated as:

- Development of a graph-neighborhood structured kernel, the vertex-degree kernel (VDK), for effectively learning the *voltage-load* function in large-scale power systems.
- A novel network-swipe Active Learning (AL) algorithm for VDK-GP that intelligently selects training data that eliminating the need for solving numerous ACPF. The proposed AL method also provides a stopping criteria without requiring out-of-sample testing, that facilitating its use for operational risk assessment.
- A conservative probabilistic bound on expected estimation error which establishes VDK-GP's statistical equivalence with ACPF based risk estimation up to the same error threshold. We demonstrate the proposed GP-based model reduces the computational burden in achieving this probabilistic bound.

To evaluate the proposed method, we conduct benchmark experiments on medium to large-sized power networks, considering uncertain loads at all load buses. Our findings demonstrate that: a) VDK-GP achieves comparable accuracy with less than 50% of the samples required by standard kernel GP; b) AL with VDK-GP achieves target model accuracy with fewer data points than VDK-GP; and c) The proposed model can be probabilistically guaranteed to achieve a similar level of accuracy as ACPF-based MCS while requiring 15 times less computational time.

The remainder of this paper is organized as follows. In Section II, we provide a brief overview of the power flow learning and we present the proposed VDK-GP and reduced representation of VDK. In Section III, we describe the idea of information gain, outline challenges in designing AL methods and the proposed network-swipe AL algorithm. In Section IV, we present the results for benchmark experiments and uncertainty quantification for medium to large systems and discuss insights. Finally, in Section V, we conclude the paper and discuss future work.

II. VOLTAGE RISK ASSESSMENT

Notation: Consider a power grid $\mathcal{G} = (\mathcal{B}, \mathcal{E})$ with \mathcal{B} denoting the set of buses/nodes and \mathcal{E} denoting the set of transmission lines/edges with impedances $R_{ij} + jX_{ij}$ per edge (ij) . We denote the complex node voltage as $v_j = V_j \angle \theta_j$ with magnitude V_j and phase angle θ_j . We denote load in the net-form i.e. *power demand* – *power generation* = *load*¹ and refer to complex power as $s_j = [p_j; q_j]$. Here, p_j (q_j) is real (reactive) load at j -th node. The space of loads is denoted by sub-space \mathcal{S} . The following AC PF equations represent the set of voltages as an implicit function of the nodal injections:

$$\forall j \in \mathcal{B}, s_j = \sum_{i:(ij) \in \mathcal{E}} v_j * (v_j^* - v_i^*) / (R_{ij} + jX_{ij}) \quad (1)$$

In power system operations, risk assessment involves evaluating the risk of constraint violation under load uncertainties in

\mathcal{S} , given a generator policy (i.e. dispatch \mathbf{p}_g^o and participation factor α). Formally, we define voltage risk assessment (VRA) as follows:

Voltage Risk Assessment Problem: *Given dispatch decision set $\{\mathbf{p}_g^o, \alpha\}$, and node voltage limits, what is the expected value by which a node voltage $V(\mathbf{s})$, with $\mathbf{s} \in \mathcal{S}$ and having probability distribution $\mathcal{P}(\mathbf{s})$, will exceed (or fall short) of limit? Mathematically, VRA, with $\Delta_V = \underline{V} - V(\mathbf{s})$ (for lower limit $V(\mathbf{s}) - \bar{V}$, is given by*

$$\text{VRA} : \mathbb{E}[h(\Delta_V(\mathbf{s})) | \mathbf{s} \in \mathcal{S}]. \quad (2)$$

Here, $\mathbb{E}[\cdot]$ is the expectation operator. Note that if $h(\cdot)$ is an identity function i.e. $h(\Delta_V) = \Delta_V$ (with \mathbf{s} omitted for brevity), then VRA models expected constraint violation Δ_V [21]. On the other hand, taking VRA to be $\max(0, \Delta_V)$ can model the average size of violation.

Nonetheless, it is challenging to compute the VRA as voltage in Eq. 1 is an *implicit non-linear function*. This is further complicated when renewable sources and variable loads like EVs are involved, such that we load is sampled from the set \mathcal{S} and load distribution $\mathcal{P}(\mathbf{s})$ does not follow a well-defined analytical distribution. This negates the possibility of using robust optimization formulation to calculate maximum node voltage with load uncertainty sub-space \mathcal{S} [22]. The alternative approach is to compute the risk empirically using a high number of AC-PF solutions for load uncertainty samples. As an illustrative example, consider the problem of violation estimation for a system, within an error margin of 10^{-3} pu (0.1% for a 1000kV system). For a 95% confidence in the estimate, the required number of PF solutions² is greater than 8×10^5 . Solving such a large number of power flows for realistic transmission network with thousand plus buses, within a time-constraint of 1 – 5 minutes³ is computationally prohibitive [1].

A prominent way to solve the risk-assessment problem is probabilistic power flow (PPF) [23], [24], where upon estimating the output distribution (e.g. node voltage magnitude), probability of violation is calculated. A variety of methods for PPF and risk-estimation use numerical methods that revolve around the Monte-Carlo Simulation (MCS) methods [25]. The MCS-based PPF works rely on numerous simulations and majority of works propose different sampling methods and Quasi-MCS methods [24], [26] to improve computational complexity. However, to achieve the statistical guarantee for arbitrary input injections, the computational burden is very high as shown in Fig. 1. Other type of numerical methods are approximation methods such as point estimate method (PEM) [27], [28]. They suffer similar limitations as MCS and estimation of complete distribution is difficult due to the requirement of the series expansion method [23]. Further, risk-estimation using PEM-based approaches does not provide any guarantee [28]. Other techniques include analytical methods such as Gaussian mixture approximation [29], and cumulant methods [30]. Although these analytical method provide better understanding of system behavior under uncertainty, they require

²as prescribed by estimation theory

³interval between consecutive real-time SCEDs

¹This is only a convention adopted and does not affect the model.

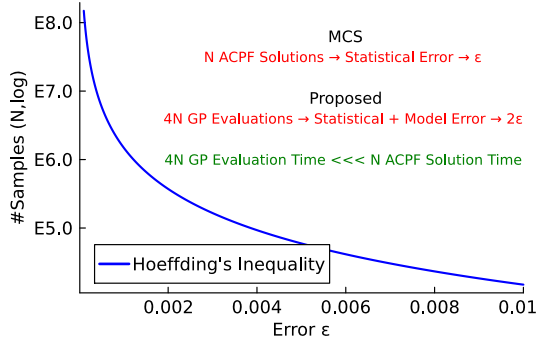


Fig. 1. Relationship between required number of samples N and error ϵ for MCS based VRA. Our proposed approach replaces these N ACPF solutions with $4N$ GP model evaluations to achieve error of same order. The key advantage lies in the fact that GP evaluations are much faster than solving ACPF, due to GP model's closed-form. For example, it takes ≈ 4205 sec for obtaining 20050 ACPF solutions, while 82000 GP evaluations takes only ≈ 33.2 sec, which corresponds to a **speedup greater than 120x**.

convolution, various transforms which are time consuming, particularly under correlated uncertain inputs. Additionally, most of these methods are developed for a particular type of input uncertainty, thus difficult to generalize.

To overcome this computational bottleneck, we propose a novel Gaussian Process (GP) based explicit model for voltages as a function of input loads, that can be (a) accurately estimated/learned using limited training data, and consequently, (b) used for fast VRA computation within a fraction of the time required for standard PF-based MCS approaches as highlighted in Fig. 1. Crucially, we are able to reinforce our extensive simulation results with theoretical bounds on the sample requirement for GP-based VRA computation, and prove its correctness using statistical estimation theory. The next section introduces our proposed Vertex-Degree Kernel based Gaussian Process that uses characteristics of power flow physics to efficiently learn AC voltages, compared to alternate data-driven approaches.

III. VERTEX-DEGREE KERNEL GAUSSIAN PROCESS (VDK-GP) FOR VOLTAGE LEARNING

This section begins by reviewing PF in functional form and describing a standard Gaussian Process model for estimating voltage. Our proposed model, VDK-GP, is described subsequently. For modeling, we describe output voltage as a function of the input load vector as:

$$V_j(\mathbf{s}) = f_j(\mathbf{s}) + \varepsilon \quad (3)$$

where, $V_j(\mathbf{s})$ is j -th node voltage measurement for load (active and reactive) vector \mathbf{s} and $f_j(\mathbf{s})$ is the unknown underlying function with $\varepsilon \sim \mathcal{N}(0, \sigma_n^2)$ being i.i.d. Gaussian noise. In Gaussian Process (GP), we consider that function f (sub-script j omitted for brevity) belongs to a zero mean Gaussian distribution [13] i.e.

$$f(\mathbf{s}) \sim \mathcal{GP}(\mathbf{0}, K(S, S)) \quad (4)$$

with $K(\cdot, \cdot)$ defining the covariance matrix or kernel matrix over the training samples and $S = [\mathbf{s}^1 \dots \mathbf{s}^i \dots \mathbf{s}^N]$ being *design matrix* having N load vector samples from training set $\{\mathbf{s}^i, V^i\}_{i=1}^N$. The kernel matrix K is constructed using

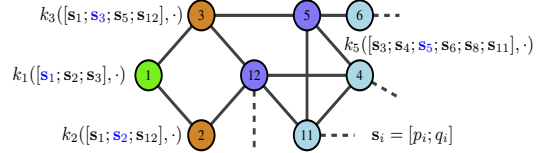


Fig. 2. A part of 118-Bus system showing the idea of vertex degree kernel construction via working over loads of a given nodes and its immediate neighbors. In Eq. (8), we use \mathbf{x}_b to represents all the load variables in b -th sub-kernel as $k_1(\mathbf{x}_1, \cdot) = k_1(\mathbf{s}_1, \mathbf{s}_2, \mathbf{s}_3, \cdot)$. For brevity, second input element in kernel function is represented using (\cdot) .

covariance or kernel function working over the load vectors at different samples, i.e. the i, j -th element $K_{i,j} = k(\mathbf{s}^i, \mathbf{s}^j)$, (see [13] for details). As voltage is a smooth function of loads, *square exponential kernel* has been extensively used for PF learning [5], [18], [31], [32]. The *square exponential kernel* is defined as

$$k(\mathbf{s}^i, \mathbf{s}^j) = \tau^2 \exp \left\{ \frac{-\|\mathbf{s}^i - \mathbf{s}^j\|^2}{2\ell^2} \right\}, \quad (5)$$

where $\|\cdot\|$ is the Euclidean norm. The *square exponential kernel* has two *hyper-parameters* $\theta = \{\tau, \ell\}$, which are selected by maximizing the marginal log likelihood (MLL) for exact inference [13]. This MLL maximization aims to find the optimal set of hyperparameters that best fit the observed data while penalizing complex models, thereby striking a balance between model complexity and goodness of fit [13]. Upon learning, the GP provides mean and variance predictions of the function as

$$\mathbb{E}[f(\mathbf{s})] = \mu_f(\mathbf{s}) = \mathbf{k}^T [K + \sigma_n^2 I]^{-1} \mathbf{V} \quad (6)$$

$$\mathbb{V}[f(\mathbf{s})] = \sigma_f^2(\mathbf{s}) = k(\mathbf{s}, \mathbf{s}) - \mathbf{k}^T [K + \sigma_n^2 I]^{-1} \mathbf{k} \quad (7)$$

Here, \mathbf{V} is the training voltage vector and $K = K(S, S)$ is the estimated kernel matrix over samples of S . The vector $\mathbf{k} = [k(\mathbf{s}^1, \mathbf{s}) \dots k(\mathbf{x}^N, \mathbf{s})]$ is obtained by applying the kernel function over \mathbf{s} and S ⁴. Note that GP not only provides point prediction as $\mu_f(\mathbf{s})$ Eq. (6), but also gives confidence level via predictive variance $\sigma_f^2(\mathbf{s})$.

It is worth noting that the MLL for the standard Squared exponential kernel is done over a $2|\mathcal{B}|$ dimensional space (double of system size), and requires a high number of samples for accurate learning. Further, if kernel design problem is solved using optimization, the overall process becomes computationally expensive [31]. In the next section, we introduce a novel GP Kernel inspired by the network structure and locality of voltages, that is able to reduce the training sample requirement for voltages, without sacrificing its accuracy.

A. Proposed Kernel Design

We design an additive GP kernel using sub-kernels, each being a squared exponential-kernel limited to the neighborhood of a nodal load, i.e., for node j we have set $\mathbf{x}_j = \{\mathbf{s}_i | i = j \text{ or } (ij) \in \mathcal{E}\}$. The intuition behind the proposed kernel design is that a node's voltage is affected by all loads but their *correlated effect*⁵ is limited to loads that are near

⁴See appendix in [5] for more details.

⁵'correlated' effect is the change in voltage due to simultaneous change in two or more nodal loads.

one another. In other words, effect of two far-away loads on nodal voltages can be considered uncorelated/independent. As maximum degree of a node is much less than the size of a power grid, each sub-kernel is low-dimensional. The complete additive kernel, the sum of these sub-kernels, is termed as Vertex Degree Kernel (VDK), and is defined as

$$k_v(\mathbf{s}^i, \mathbf{s}^j) = \sum_{b=1}^{|\mathcal{B}|} k_b(\mathbf{x}_b^i, \mathbf{x}_b^j) \quad (8)$$

Here, $k_b(\mathbf{x}_b^i, \mathbf{x}_b^j)$ is the sub-kernel working over $\mathbf{x}_b \subset \mathbf{s}$. Note that by relying on the grid structure, neighborhood based correlations are kept intact in VDK, but complex design choices for kernels are avoided. Fig. 2 shows the idea of VDK construction. Each sub-kernel $k_b(\cdot, \cdot)$ has hyper-parameters θ_b that form the full hyper-parameter vector for VDK as $\theta = [\theta_1, \dots, \theta_{|\mathcal{B}|}]$. As the sum of valid kernel functions is a kernel function, standard exact inference can be performed via optimizing MLL using $k_v(\cdot, \cdot)$ [13], [33], [34]. However, as *square exponential kernel* has two hyper-parameters (5), the total number of hyper-parameters in VDK (8) will be twice the number of network nodes. In the next section, we show that the neighborhood based additive form of VDK lends itself to a simple active learning algorithm for fast hyperparameter estimation.

IV. ACTIVE LEARNING FOR VDK-GP

We are interested in rapid estimation of $f(\mathbf{s})$ (j -th node's voltage function) in Eq. 4 by learning the hyper-parameter θ , and further in determining a tractable stopping criterion for terminating the learning that does not rely on computationally expensive out of sample AC-PF solutions.

To answer the first part, we propose an active learning (AL) [19] mechanism that sequentially selecting training samples to maximize the information about the voltage function, and predictive variance as an indicator to terminate the learning process. In GP modeling (or Bayesian setting in general) 'information gain' is used as a measure to quantify the informativeness of a training set or sample. Let, $\mathcal{A} \subset \mathcal{L}$ where \mathcal{L} is the complete training set or space. The Information gained by samples in \mathcal{A} is the information theoretic mutual information between voltage function f and $\mathbf{V}_{\mathcal{A}}$ (vector of voltage samples following Eq. (3)) [35], and is given by $I(\mathbf{V}_{\mathcal{A}}; f) = (1/2) \log |I + \sigma_\epsilon^{-2} K_{\mathcal{A}}|$. Here $K_{\mathcal{A}}$ is the kernel matrix constructed using samples in set \mathcal{A} . Importantly, finding the best \mathcal{A} with given cardinality $|\mathcal{A}| < |\mathcal{L}|$ is an *NP-hard* problem [35]. However, two results facilitate tractable AL. First, in [36] information gain has been shown to be a *submodular* function of set \mathcal{A} , implying that greedy algorithm for sample selection is at least within $\sim 63\%$ of optimal solution. Second, the information gain in a new sample s is given by predictive variances Eq. (7). Hence, the next training sample, for j -th node voltage function learning, can be obtained by solving

$$\mathbf{s}^{t+1} = \arg \max_{\mathbf{s} \in \mathcal{L}} [\sigma_f^t(\mathbf{s})]^2 \quad (9)$$

Here, $\sigma_f^t(\cdot)$ is predictive standard deviation of the GP trained on first t samples, as given by Eq. (7). As eluded in the

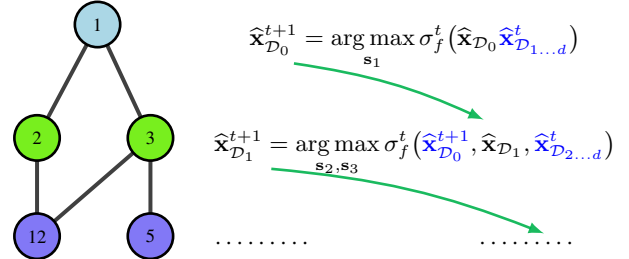


Fig. 3. Description of steps within $(t+1)^{\text{th}}$ iteration of network-swipe Algorithm 1 for AL. At each step, only loads at a fixed graph distance from j are treated as variables (colored in black) for information maximization, while others are kept fixed (colored in blue). For example, $\bar{\mathbf{x}}_{\mathcal{D}_1} = \{\mathbf{s}_2, \mathbf{s}_3\}$. Once those loads are optimized, their values are updated before the next step. In second step, updated output of the first step $\hat{\mathbf{x}}_{\mathcal{D}_0}^{t+1}$ are used along with values from previous iteration at all other loads $\hat{\mathbf{x}}_{\mathcal{D}_2, \dots, d}^t$, as given in Eq. (10).

introduction, for large networks, the non-convex function makes Eq. (9) quickly intractable for standard GP [5], as the input vector in Kernels has size $2|\mathcal{B}|$ [37]. While VDK is separable in terms of lower-dimensional sub-kernels k_b given in Eq. (8), they have overlapping input groups for any two sub-kernels k_{b_i}, k_{b_j} at nodes i, j that are within two graph hops. This means that a simple parallelization into sub-kernels isn't possible for AL. Instead, we propose a block-descent type iterative network-swipe algorithm to exploit VDK's form for optimizing Eq. (9). At each iteration t of the network-swipe algorithm, at the first step, we solve Eq. (9) with respect to \mathbf{x}_j^t (load at the node where voltage is being predicted), while keeping all other loads fixed. The load at j is updated with the optimized value. In the second step, we solve Eq. (9) for all loads at nodes i such that $(ij) \in \mathcal{E}$ (1 hop neighbors of j). All other loads are kept unchanged. In the next step, loads at two-hop neighbors of j are chosen to solve Eq. (9), and so on till all loads have been updated. For elucidation, we use $\mathcal{D}_r^j, 0 \leq r \leq d$ to denote distinct node groups at a graph distance of r from node j , with max-distance d . Hence, $\mathcal{D}_0^j = \{j\}$, while $\mathcal{D}_r^j = \{i : (\mathcal{D}_{r-1}^j, i) \in \mathcal{E}\}$. Mathematically, the t^{th} iteration of network-swipe solves the following non-linear optimization problems sequentially for $i = 0, 1 \dots d$

$$\hat{\mathbf{x}}_{\mathcal{D}_i}^{t+1} = \arg \max_{\hat{\mathbf{x}}_{\mathcal{D}_i} \in \mathcal{L}_i} \sigma_f^t(\hat{\mathbf{x}}_{\mathcal{D}_0, \dots, i-1}^{t+1}, \hat{\mathbf{x}}_{\mathcal{D}_i}, \hat{\mathbf{x}}_{\mathcal{D}_{i+1}, \dots, d}^t) \quad (10)$$

Here, $\hat{\mathbf{x}}_{\mathcal{D}_i} = \{\mathbf{s}_j | j \in \mathcal{D}_i\}$. Also, \mathcal{L}_i represents the hypercube slice with respect to loads present in $\hat{\mathbf{x}}_{\mathcal{D}_i}$. The algorithm then starts a new iteration $(t+1)^{\text{th}}$ to determine the next sample. The pseudo-code for AL is listed in Algorithm 1 and a graphical representation of steps for target node j is shown in Fig. 3.

In Algorithm 1, we have used a time budget of T_{max} , and a predictive variance threshold of $\sigma_{threshold}^2$. While we present a single sequence of network swipe steps to determine the next injection sample s^t , multiple swipes can be performed across network to improve the information gain in s^t . Further, for solving Eq. (10), in Algorithm 1 we use function evaluation with different batch sizes and select the best candidate of injection among the random samples. Further, the function evaluation-based approach will allow to build parallelizable optimization methods, helping to scale and improve performance of the proposed network-swipe AL in future works. In

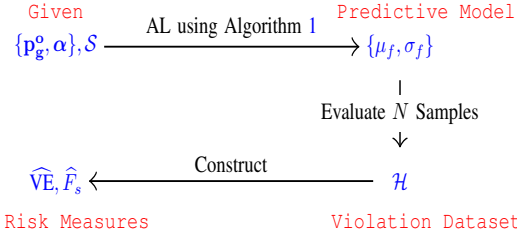


Fig. 4. Flowchart of risk measure calculation using AL-VDK based voltage learning. Here, $\mathcal{H} = \{h_m(\Delta_V^i)\}_{i=1}^N$ and \hat{F}_s is the cumulative density function (CDF) of violation $h_m(\Delta_V)$ random variable. This is then used directly to estimate probability of voltage violation $\mathbb{P}\{h_m(s) > 0\}$.

the next section, we provide guarantees on using VDK-GP for risk estimation in the grid.

It is crucial to emphasize the effectiveness of the proposed network-swipe AL method, which is also related to the incorporation of the VDK structure. This Algorithm 1 enables the optimization problem, as defined in (10), to remain low-dimensional. Utilizing a conventional GP kernel, standard active learning methods typically encounter the curse of dimensionality during sample-based optimization, particularly when seeking maximum variance across a load space of dimension $2|\mathcal{B}|$, where $|\mathcal{B}|$ denotes the number of buses within the system. Consequently, the proposed network-swipe AL design requires sample-based optimization over load variables set at a particular depth (defined as \mathcal{D}_r^j) at a time. This low-dimensionality of optimization is particularly advantageous for applying proposed active learning method to large-scale networks.

V. GUARANTEES ON RISK ASSESSMENT USING VDK-GP

As discussed in Section II and Fig. 1, empirical voltage risk assessment (VRA) using MCS of power flow samples is computationally expensive, but faster using VDK-GP due to its closed-form input-output map. Fig. 4 presents the complete idea of risk assessment by first estimating the VDK-GP to generate voltage samples and determining the empirical violation estimation (VE) as well as CDF of the violation. While we demonstrate the computational performance in the next section, we address the question of theoretical guarantee on the performance of VDK-GP for VRA. We first derive results for general ML-based methods and extend it to VDK-GP (VE and CDF of violation) as a special case of a ML model. Consider a function $h(\cdot)$ defined over node voltage

V . Let $h_p(s) = h(V(s))$ indicate its evaluation at voltage $V(s)$ derived from solving NRLF at load s , and let $h_m(s) = h(\hat{V}(s))$ denote its evaluation for voltage derived from a ML predictor (e.g. GP, DNN etc.) at s . We then have the following result.

Theorem 1. Expected Value Estimation Error Bound: Suppose that a given ML model with output \hat{V} satisfies

$$\mathbb{P}\{|V(s^i) - \hat{V}(s^i)| > \varepsilon_m\} \leq \delta \quad (11)$$

with $\delta \in (0, 1)$ for any $s \in \mathcal{S}$. Let $h(\cdot)$ be a Lipschitz continuous function with Lipschitz constant L . Then the error in estimating h with the ML model with N samples is bounded with probability greater than $1 - \beta$ as

$$|\mathbb{E}[h_p(s)] - \hat{\mathbb{E}}[h_m(s)]| \leq L\varepsilon_m + 2M\delta + \varepsilon_h \quad (12)$$

where, $\beta \in (0, 1)$, $\varepsilon_h = \sqrt{\frac{4M^2 \log(2/\beta)}{N}}$, M is a uniform bound on the maximum error that satisfies $-M < h(s) < M$, and N is number of samples.

Here, $\hat{\mathbb{E}}[\cdot]$ is the empirical estimate of expectation using N samples. The detailed proof is given in the Appendix A. Theorem 1 states that if an ML model is accurate in estimating V (voltage magnitude), then empirical estimation of expected violation using the ML-generated samples is close to the true expected violation. Further, the use of ML has potential computational speed-up since direct function evaluation is significantly faster than solving traditional ACPF for each sample. Consider the case where h is given by the Sigmoid function to convert deviation from voltage limit Δ_V calculated using power flow solution as

$$h_p(s) = \frac{e^{\Delta_V(s)}}{1 + e^{\Delta_V(s)}} - 0.5 \quad (13)$$

Note that Sigmoid function has Lipschitz constant equal to one, and provides information about both extent of violation as well as level of security. We subtract 0.5 so that $h_p(s) > 0$ implies violation. Theorem 1 provides concentration or error bounds on violation estimation (2). By ensuring preservation of violation level information, the Sigmoid function allows for effective critical load point sampling [38].

Theorem 1 requires a probabilistic error bound on the ML model given in Eq. (11), but validating this bound would require extensive out-of-sample testing, through Hoeffding's inequality⁶. This poses a challenge when generating ground-truth solutions (e.g., voltage solutions from AC-PF) is difficult within the ISO's time-constraints for risk assessment. Contrary to ML models with point-prediction (e.g. DNN), GP automatically offers a measure of confidence around the mean prediction, through the predictive variance in voltage, $\sigma_f^2(s)$ [13]. This crucial feature enables GP to probabilistically upper-bound voltage solutions ($V(s)$) using mean and variance, $(\mu_f(s)$ and $\sigma_f^2(s))$ as described in Eq. 7 and eliminates the need for out-of-sample testing. The next corollary extends Theorem 1 for VRA using GP's predictive variance guarantee.

⁶Minimum number of ACPF-MCS samples N require to obtain statistical error in VRA estimation below ε , with confidence level β , is given as $N \geq 0.5 \log(2/\beta) \varepsilon^{-2}$ [39].

Algorithm 1 Network-Swipe Algorithm for AL

Require: $T, \mathcal{D}, \{s^1, V^1\}, \sigma_{threshold}^2, T_{max}$

- 1: Initialize GP model (4) with VDK (8)
- 2: **while** $\sigma_f^2(s^t) \geq \sigma_{threshold}^2$ **do**
- 3: Solve (10) for $\hat{x}_{\mathcal{D}_i}^{t+1}$, sequentially for $i = 1 \dots d$
- 4: Solve ACPF for load s^{t+1} to get V^{t+1}
- 5: Update GP model with (s^{t+1}, V^{t+1}) ; $t = t + 1$
- 6: **If** runtime $> T_{max}$ **then** break
- 7: **end while**

Output: Compute $\mu_f(s), \sigma_f^2(s)$ for final GP

Corollary 1.1. Suppose that the GP assumption holds for PF such that voltage values, for any two arbitrary load vectors, are jointly Gaussian. Then, $\mathbb{P}\{|V(\mathbf{s}) - \widehat{V}(\mathbf{s})| \geq \varepsilon_m\} \leq \delta(\kappa)$ where $\widehat{V}(\mathbf{s}) = \mu_f(\mathbf{s}^i) \pm \kappa\sigma_f(\mathbf{s})$ for any $\varepsilon_m > 0$. And with $h(\cdot)$ being Sigmoid function, error in VE using GP is probabilistically bounded as

$$\mathbb{P}\left\{|VE - \widehat{VE}| < \varepsilon_m + 2M\delta(\kappa) + \varepsilon_h\right\} \geq 1 - \beta$$

where, definitions of variables are same as in Theorem 1 and $\delta(\kappa)$ is expected fraction of voltage values outside the range given by $\mu_f(\mathbf{s}^i) \pm \kappa\sigma_f(\mathbf{s})$.

The proof follows directly from Theorem 1 and properties of Gaussian distribution. Note that in Corollary 1.1, the GP model error probability δ is a function of variance multiplier κ in \widehat{V} . The value of $\delta(\kappa)$ decreases rapidly with increase in κ values. At $\kappa = 2$ we have $\delta(\kappa) \approx 0.05$ while $\kappa = 4$ will give $\delta(\kappa) \approx 6.334 \times 10^{-7}$. As discussed in Fig. 1, performing the estimation by solving AC-PF over multiple load samples is not feasible due to high computational burden. Using $N > 820,000$ in Hoeffding's inequality [39] and conditions in Corollary 1.1, we will have $\varepsilon_h = 3 \times 10^{-3} = \varepsilon_m^7$ and confidence of 95% ($\beta = 0.05$). Further, using $\delta(\kappa) = 6.334 \times 10^{-7}$ and $M = 1^8$, the VE will be bounded as $|\mathbb{E}[h_p(\mathbf{s})] - \widehat{\mathbb{E}}[h_m(\mathbf{s})]| \leq 6.001 \times 10^{-3}$. To generate same accuracy using AC-PF samples, we will require 205,000 NRLF solutions that is much more computationally expensive.

Additionally, we can use AL-VDK GP to generate the empirical CDF \widehat{F}_s of violation $h_m(\Delta_V)$. This CDF can provide information on the probability of violation (PoV). formalized below.

Probability of Violation: Given dispatch decision set $\{\mathbf{p}_g^o, \alpha\}$, and node voltage limit \underline{V} , PoV is defined as

$$\mathbb{P}_S\{h(\Delta_V) > 0\}. \quad (14)$$

For AL-VDK model's applicability, it is important to have confidence that the procedure in Fig. 4 will not underestimate the PoV. We present the theorem below which certifies that proposed GP-based predictive model will always overestimate the PoV i.e. provide a conservative estimate of security.

Theorem 2. The GP-based predictive model overestimates probability of voltage violation i.e.

$$\mathbb{P}\{h(\mathbf{s}) > 0\} \leq \widehat{\mathbb{P}}\{h_m(\mathbf{s}) > 0\}$$

with confidence $1 - \beta$.

Proof. Detailed proof is given in Appendix A \square

VI. RESULTS AND DISCUSSION

In this section, simulation results demonstrate a) that our Graph-structured kernel (VDK) (8) outperforms standard GP model [5] in voltage prediction at same sample complexity,

⁷The confidence bound of the GP is valid for any $\varepsilon_m > 0$. However, for simplicity and to maintain consistency, we chose $\varepsilon_m = \varepsilon_h$.

⁸As we use Sigmoid function (13), $M = 1$ can be used to satisfy the condition $-M < h(\mathbf{s}) < M$. More details of M are with proof of Theorem 1 in Appendix A

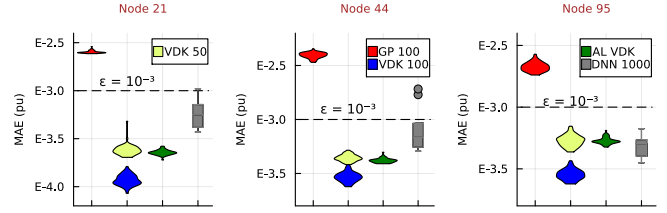


Fig. 5. Comparison of MAE performance of different methods, demonstrating the efficiency and low sample-complexity of AL-VDK, on three different nodes of 118-Bus system. GP, VDK and AL-VDK results are of 50 trials, and DNN results are of 10 trials. AL-VDK uses significantly fewer samples as dictated by Algorithm 1. AL-VDK training samples for all 50 trials are within 43 – 48, 43 – 47 and 42 – 47 for nodes 21, 44, and 95 respectively.

b) active learning (AL) with VDK (**AL-VDK**) efficiently learns voltage functions with acceptable error using fewer samples than VDK and c) AL-VDK voltage predictor exhibits significantly lower time complexity than NRLF for statistical estimation of voltage violation (VE) (Corollary 1.1), while the proposed model is a conservative estimator of risk of violation (Theorem 2). The VE value indicate the extent by which voltage goes beyond the lower voltage limits, calculated using the Sigmoid (13) function. To obtain the node voltages for given uncertainty set \mathcal{S} and decision set $\{\mathbf{p}_g^o, \alpha\}$, we use PowerModels.jl, for running ACPF. For this, upon sampling a load vector $\mathbf{s} \in \mathcal{S}$, we update the generator points in the data file using the participation factors i.e. $\mathbf{p}_g = \mathbf{p}_g^o + \alpha\Delta\mathbf{s}$ with $\Delta\mathbf{s}$ being sum of load change from base-point. To validate the model, 1000 out-of-sample testing points are used in all cases unless stated otherwise. Three different systems from pglib-library [40] are used for validation (118-Bus, 500-Bus, and 1354-Bus). We use the Square Exponential Kernel, both for standard GP and VDK-GP and model them in Julia. Additionally, we use a DNN, deep neural network, of three layers and 1000 neurons in each layer [10]⁹ for comparison. We use mean absolute error (MAE) to validate the performance of proposed models: $\text{MAE} = M^{-1} \sum_i |\mu_f(\mathbf{s}^i) - V(\mathbf{s}^i)|$ for $i = 1 \dots M$.

118-Bus System: The load space is constructed by varying individual real power loads within $\pm 10\%$ and load power factors between 0.9 times the base power factor and 1.0. Fig. 5 compares the MAE performance of four different methods: GP, VDK, DNN, and AL-VDK. First, GP fails to achieve MAE below the desired threshold of $1E - 3$ using 100 training samples. Further as shown, AL-VDK achieves competitive MAE performance while using significantly fewer training samples than the other methods. Notably, AL-VDK's sample usage is dynamically determined by Algorithm 1, leading to improved data efficiency. In contrast, DNNs require a larger set of 1,000 samples for each trial to achieve an error of the same order, highlighting their high training data requirement. Also, note that AL-VDK performs better than VDK with 50 samples, showing AL's capability to reduce MAE efficiently with an increase in training samples. The average time taken by a complete trial of the AL-VDK algorithm is 5.8 seconds (without testing) compared to 8.3 seconds for 100-sample VDK. These results demonstrate that AL-VDK offers a promising

⁹We use Flux.jl with standard settings of ADAM solver to optimize hyper-parameters. Batch size is 5 and Epochs are set as 200.

TABLE I
TRAINING SAMPLE REQUIREMENT AND RISK ESTIMATION RESULTS IN
500-BUS SYSTEM

	Training Samples	Time(s)	$\Delta VE \times 10^{-4}$
4	67 - 70	28 - 30	7.8 ± 0.5
181	71 - 76	30 - 33	8.0 ± 0.2
268	102 - 109	53 - 58	7.9 ± 0.2
320	72 - 76	30 - 33	7.8 ± 0.4
321	70 - 77	30 - 33	6.8 ± 0.5

Mean evaluation time for 82000 samples is ≈ 33.2 sec
 NRLF running time for 20500 samples is ≈ 4205 sec
 ΔVE : Difference in VE values using NRLF and AL-VDK

TABLE II
ESTIMATED VALUE PROBABILITY OF VIOLATION (POV) FOR 500-BUS
SYSTEM VOLTAGES WITH DIFFERENCE IN ESTIMATION USING AL-VDK

PoV	Node				
	4	181	268	320	321
Estimated [†]	0.0487	0.0115	0.6879	0.8092	0.9108
Difference [#]	+0.04	+0.01	+0.16	+0.15	+0.10

[†]using 82000 and mean over AL trials;

[#]between 20050 ACPF and 82000 AL-VDK evaluations

[#]Positive Difference \implies Overestimation

combination of accuracy and efficiency, making it a valuable tool for scenarios where limited ACPF data is available or acquiring PF data by running NRLFs is time-consuming.

500-Bus System: The load space is constructed by varying individual real power load within $\pm 10\%$ and load power factor between 0.95 times of base power factor and 1.0. Besides the MAE accuracy results, in this subsection we present the risk estimation results on five different node voltages. These node indices are selected as the voltages at these nodes have the highest variance among 20500 ACPF solutions. Fig. 6 compares the MAE performance of different methods GP, VDK, and AL-VDK while Table I shows details of AL-VDK result for all five nodes. Firstly, the MAE performance of AL-VDK is comparable to that of VDK even when it uses ~ 70 training samples instead of 100 used by VDK for most nodes in Fig. 6. Further, using similar number of samples, AL-VDK outperforms VDK for node 268 which has higher voltage variance. This show that at same sample complexity, the worst performing trial of AL-VDK is better than mean performance of VDK.

To calculate risk levels and ΔVE presented in Table I, we fix the target that error in violation estimation must be less than 6×10^{-2} . The estimation error here means the difference between true VE and proposed ML-based VE i.e. $|\mathbb{E}[h_p(s)] - \widehat{\mathbb{E}}[h_m(s)]|$, from Theorem 1. To estimate violation with statistical error less than 6×10^{-2} , at least 20500 NRLF solutions¹⁰ are required as per Hoeffding's inequality and 82000 AL-VDK model evaluation are needed as per Corollary 1.1. The 20500 NRLF trials took more than one hour (4205 sec.) on a Mac M1 Max with 32GB RAM. On same machine it takes only ~ 33.2 seconds to obtain 82000 voltage predictions for a node. Considering the training time and evaluation time, it takes less than 90 seconds to estimate risk levels with error ΔVE of the order 10^{-4} , which is two order of magnitude lower

¹⁰This is because $\varepsilon = 6 \times 10^{-3}$ will require more than 200000 NRLF solutions which is computationally prohibitive. Also, note that from Corollary 1.1, to achieve $|\mathbb{E}[h_p(s)] - \widehat{\mathbb{E}}[h_m(s)]| \leq 6 \times 10^{-2}$, ε_n should be set at 3×10^{-2} and thus we require 82,000 AL-VDK evaluations.

than acceptable statistical error level of 6×10^{-2} . Note that, ΔVE represents the difference between NRLF-based statistical estimation using 20500 samples and AL-VDK based statistical estimation using 82000 samples. The two order of magnitude difference in ΔVE and acceptable $|\mathbb{E}[h_p(s)] - \widehat{\mathbb{E}}[h_m(s)]|$ signifies that AL-VDK induced error in estimation will not affect the quality of the statistical estimation. Thus, NRLF samples can be replaced by AL-VDK evaluations as shown in Fig. 4. Also note that proposed method achieves ΔVE and MAE of same order.

As discussed in Section V, we would want an ML model to be conservative in risk estimation i.e. estimated probability of violation must be more using an ML model than estimated using NRLF solution. Fig. 7 shows the violation distributions and violation probability values calculated using NRLF and AL-VDK models. As blue curves are shifted towards right for all nodes, it is clear that AL-VDK overestimates the risk compares to NRLF as proved in Theorem 2. Similarly, Table II shows that difference between AL-VDK based estimation and ACPF based estimation of probability of violation is always positive. Also, results show that voltage at node 4 and node 181 are probabilistically secure, if maximum acceptable violation is considered to be 5%.

1354-Bus System: The construction of the load space is similar to that of the 500-Bus case. Table III presents the details of AL-VDK results across 10 trials on two distinct nodes. We consider a lower limit of 0.90 pu, and the node index is chosen based on a variation exceeding 0.010 pu (minimum - maximum). To manage the sample requirement, we set $\varepsilon = 10^{-1}$ due to the substantial time needed for solving ACPFs in the 1354-Bus system. In Table III, both nodes exhibit $\widehat{VE} > 0$, indicating conservativeness of the AL-VDK based estimates. Additionally, we achieve a VE difference of 10^{-4} , mirroring the outcomes in the 500-Bus system. The total time taken for learning and VE estimation is less than 200 seconds for a node, a significant reduction compared to the approximately one hour needed for solving 2050 PF solutions. Consequently, the proposed method attains a 20-fold reduction in the time complexity for obtaining VE with an error of order 10^{-4} . These results underscore the applicability of the proposed method, even for large-scale systems.

TABLE III
RISK ESTIMATION RESULTS IN 1354-BUS SYSTEM

	Samples	Time(s)	$\Delta VE \times 10^{-4}$
183	77 - 81	159 - 168	8.0 ± 0.5
287	77 - 81	154 - 164	8.2 ± 0.2

Mean evaluation time for 8200 samples is ≈ 29.8 sec
 NRLF running time for 2050 samples is ≈ 3879 sec
 ΔVE : Difference in VE using NRLF and AL-VDK

VII. CONCLUSION

This paper introduces a novel graph-structured kernel, the vertex degree kernel (VDK), designed to estimate violation risk using Gaussian Process (GP) with an additive structure inspired by physics. VDK effectively leverages network graph information, providing a promising approach for improved voltage-load relationship modeling. The results obtained demonstrate the superiority of VDK-GP over the full

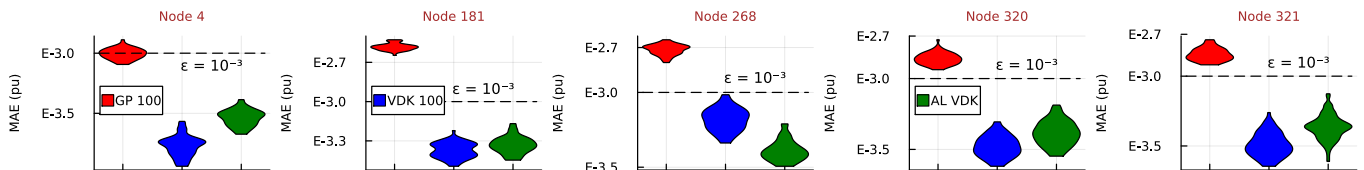


Fig. 6. Comparison of MAE performance of different methods, demonstrating the efficiency and low sample-complexity of AL-VDK, on three different nodes of 500-Bus system. AL-VDK uses significantly fewer samples as dictated by Algorithm 1 and details are given in Table I. Our target is to achieve $MAE < 10^{-3}$ (0.1% error for a 1000kV system), and ACPF samples are generated till that threshold is reached.

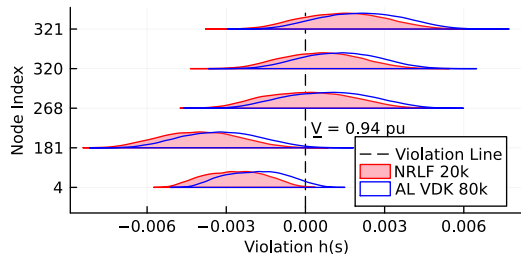


Fig. 7. Distributions of violation $h(s)$ obtained using 20050 NRLF solutions and 82000 AL-VDK evaluations after a using a random training instance. The right hand side shift of blue distributions shows that proposed AL-VDK always provides an overestimation of risk, as proven in Theorem 2.

GP, showcasing a substantial reduction in sample complexity. Also, the proposed network-swipe AL algorithm further enhances model performance by employing intelligent data selection, maximizing information gain without reliance on labeled data. Results show that proposed method achieves more than 10 fold reduction in time complexity to perform risk estimation with error $\sim 10^{-4}$ while conservatively overestimating the probability of violation. Both these provide numerical evidence to support the theoretical results presented in the paper. For future directions, the additive structure and active learning capabilities of VDK-GP pave the way for developing Bayesian optimization-based methods tailored for large-scale power systems.

REFERENCES

- [1] N. Barry *et al.*, “Risk-aware control and optimization for high-renewable power grids,” *arXiv preprint arXiv:2204.00950*, 2022.
- [2] J. D. McCalley *et al.*, “Voltage risk assessment,” in *1999 IEEE Power Engineering Society Summer Meeting*, vol. 1. IEEE, 1999, pp. 179–184.
- [3] X. Wang, R.-P. Liu, X. Wang, Y. Hou, and F. Bouffard, “A data-driven uncertainty quantification method for stochastic economic dispatch,” *IEEE Trans. on Power Systems*, vol. 37, no. 1, pp. 812–815, 2022.
- [4] J. J. Grainger and W. D. Stevenson, *Power System Analysis*, 2003.
- [5] P. Pareek and H. D. Nguyen, “A framework for analytical power flow solution using gaussian process learning,” *IEEE Trans. on Sustainable Energy*, vol. 13, no. 1, pp. 452–463, 2021.
- [6] B. Stott, J. Jardim, and O. Aisaç, “Dc power flow revisited,” *IEEE Trans. on Power Systems*, vol. 24, no. 3, pp. 1290–1300, 2009.
- [7] D. K. Molzahn, I. A. Hiskens *et al.*, “A survey of relaxations and approximations of the power flow equations,” *Foundations and Trends® in Electric Energy Systems*, vol. 4, no. 1-2, pp. 1–221, 2019.
- [8] G. E. Karniadakis *et al.*, “Physics-informed machine learning,” *Nature Reviews Physics*, vol. 3, no. 6, pp. 422–440, 2021.
- [9] B. Huang and J. Wang, “Applications of physics-informed neural networks in power systems - a review,” *IEEE Trans. on Power Systems*, vol. 38, no. 1, pp. 572–588, 2023.
- [10] M. Gao *et al.*, “A physics-guided graph convolution neural network for optimal power flow,” *IEEE Trans. on Power Systems*, 2023.
- [11] X. Hu, H. Hu, S. Verma, and Z.-L. Zhang, “Physics-guided deep neural networks for power flow analysis,” *IEEE Trans. on Power Systems*, vol. 36, no. 3, pp. 2082–2092, 2020.
- [12] K. Chen and Y. Zhang, “Physics-guided residual learning for probabilistic power flow analysis,” *arXiv preprint arXiv:2301.12062*, 2023.
- [13] C. K. Williams and C. E. Rasmussen, *Gaussian processes for machine learning*. MIT press Cambridge, MA, 2006, vol. 2, no. 3.
- [14] M. Jalali *et al.*, “Inferring power system dynamics from synchrophasor data using gaussian processes,” *IEEE Trans. on Power Systems*, vol. 37, no. 6, pp. 4409–4423, 2022.
- [15] P. Pareek and H. D. Nguyen, “Gaussian process learning-based probabilistic optimal power flow,” *IEEE Trans. on Power Systems*, vol. 36, no. 1, pp. 541–544, 2020.
- [16] M. Mitrovic *et al.*, “Data-driven stochastic ac-opf using gaussian process regression,” *International Journal of Electrical Power & Energy Systems*, vol. 152, p. 109249, 2023.
- [17] M. K. Singh *et al.*, “Physics-informed transfer learning for voltage stability margin prediction,” in *2023 IEEE International Conference on Acoustics, Speech and Signal Processing (ICASSP)*, 2023, pp. 1–5.
- [18] Y. Xu *et al.*, “Probabilistic power flow based on a gaussian process emulator,” *IEEE Trans. on Power Systems*, vol. 35, no. 4, pp. 3278–3281, 2020.
- [19] B. Settles, “Active learning literature survey,” 2009.
- [20] C. Riis *et al.*, “Bayesian active learning with fully bayesian gaussian processes,” *Advances in Neural Information Processing Systems*, vol. 35, pp. 12 141–12 153, 2022.
- [21] M. Ni *et al.*, “Online risk-based security assessment,” *IEEE Trans. on Power Systems*, vol. 18, no. 1, pp. 258–265, 2003.
- [22] D. K. Molzahn and L. A. Roald, “Grid-Aware versus Grid-Agnostic Distribution System Control: A Method for Certifying Engineering Constraint Satisfaction,” in *52nd Hawaii International Conference on System Sciences (HICSS)*, January 2019.
- [23] B. R. Prusty and D. Jena, “A critical review on probabilistic load flow studies in uncertainty constrained power systems with photovoltaic generation and a new approach,” *Renewable and Sustainable Energy Reviews*, vol. 69, pp. 1286–1302, 2017.
- [24] K. N. Hasan, R. Preece, and J. V. Milanović, “Existing approaches and trends in uncertainty modelling and probabilistic stability analysis of power systems with renewable generation,” *Renewable and Sustainable Energy Reviews*, vol. 101, pp. 168–180, 2019.
- [25] R. N. Allan and A. L. Da Silva, “Probabilistic load flow using multilinearizations,” in *IEE Proceedings C (Generation, Transmission and Distribution)*, vol. 128, no. 5. IET, 1981, pp. 280–287.
- [26] H. Yu, C. Chung, K. Wong, H. Lee, and J. Zhang, “Probabilistic load flow evaluation with hybrid latin hypercube sampling and cholesky decomposition,” *IEEE Transactions on Power Systems*, vol. 24, no. 2, pp. 661–667, 2009.
- [27] J. M. Morales and J. Perez-Ruiz, “Point estimate schemes to solve the probabilistic power flow,” *IEEE Trans. on power systems*, vol. 22, no. 4, pp. 1594–1601, 2007.
- [28] X. Li, X. Zhang, L. Wu, P. Lu, and S. Zhang, “Transmission line overload risk assessment for power systems with wind and load-power generation correlation,” *IEEE Transactions on Smart Grid*, vol. 6, no. 3, pp. 1233–1242, 2015.
- [29] M. Nijhuis, M. Gibescu, and S. Cobben, “Gaussian mixture based probabilistic load flow for lv-network planning,” *IEEE Transactions on Power Systems*, vol. 32, no. 4, pp. 2878–2886, 2016.
- [30] C. Lin, Z. Bie, C. Pan, and S. Liu, “Fast cumulant method for probabilistic power flow considering the nonlinear relationship of wind power generation,” *IEEE Transactions on Power Systems*, vol. 35, no. 4, pp. 2537–2548, 2019.
- [31] J. Liu and P. Srikantha, “Kernel structure design for data-driven probabilistic load flow studies,” *IEEE Trans. on Smart Grid*, vol. 13, no. 4, pp. 2679–2689, 2022.
- [32] Y. Xu *et al.*, “A data-driven nonparametric approach for probabilistic load-margin assessment considering wind power penetration,” *IEEE Trans. on Power Systems*, vol. 35, no. 6, pp. 4756–4768, 2020.
- [33] X. Lu *et al.*, “Additive gaussian processes revisited,” in *International Conference on Machine Learning*. PMLR, 2022, pp. 14 358–14 383.

- [34] D. K. Duvenaud *et al.*, “Additive gaussian processes,” *Advances in neural information processing systems*, vol. 24, 2011.
- [35] N. Srinivas *et al.*, “Information-theoretic regret bounds for gaussian process optimization in the bandit setting,” *IEEE Trans. on Information Theory*, vol. 58, no. 5, pp. 3250–3265, 2012.
- [36] A. Krause and C. E. Guestrin, “Near-optimal nonmyopic value of information in graphical models,” *arXiv preprint arXiv:1207.1394*, 2012.
- [37] P. I. Frazier, “A tutorial on bayesian optimization,” *arXiv preprint arXiv:1807.02811*, 2018.
- [38] A. Lukashevich, A. Bulkin, R. Grinin, I. Makarov, and Y. Maximov, “Importance sampling approach for dynamic stochastic optimal power flow control,” *arXiv preprint arXiv:2310.02509*, 2023.
- [39] W. Hoeffding, “Probability inequalities for sums of bounded random variables,” *The collected works of Wassily Hoeffding*, pp. 409–426, 1994.
- [40] S. Babaeinejadzarookolae *et al.*, “The power grid library for benchmarking ac optimal power flow algorithms,” *arXiv preprint arXiv:1908.02788*, 2019.

APPENDIX A PROOFS

A. Proof of Theorem 1

Proof. The expression in the theorem can be written as

$$\begin{aligned} & |\mathbb{E}[h_p(\mathbf{s})] - \widehat{\mathbb{E}}[h_m(\mathbf{s})]| \\ &= |\mathbb{E}[h_p(\mathbf{s})] - \mathbb{E}[h_m(\mathbf{s})] + \mathbb{E}[h_m(\mathbf{s})] - \widehat{\mathbb{E}}[h_m(\mathbf{s})]| \\ &\leq \underbrace{|\mathbb{E}[h_p(\mathbf{s})] - \mathbb{E}[h_m(\mathbf{s})]|}_{\equiv B} + \underbrace{|\mathbb{E}[h_m(\mathbf{s})] - \widehat{\mathbb{E}}[h_m(\mathbf{s})]|}_{\equiv C} \end{aligned} \quad (15)$$

Using Jensen’s inequality, we can upper bound B as follows

$$B \leq \mathbb{E}[|h_p(\mathbf{s}) - h_m(\mathbf{s})|] \leq \int_{\mathcal{S}} |h_p(\mathbf{u}) - h_m(\mathbf{u})| \mathcal{P}(\mathbf{u}) d\mathbf{u} \quad (16)$$

Under the theorem’s assumption, $h(\cdot)$ is a Lipschitz continuous function with Lipschitz constant L , and M is a uniform bound satisfying $M > h_p(\mathbf{s})$. Using the assumption on the ML model’s performance, i.e., $\mathbb{P}\{|V(\mathbf{s}) - \widehat{V}(\mathbf{s})| > \varepsilon_m\} \leq \delta_\varepsilon$ for $\varepsilon_m > 0$ and $\delta_\varepsilon \in (0, 1)$, we have for any $\varepsilon > 0$,

$$\begin{aligned} & \mathbb{P}\{|h_p(\mathbf{s}) - h_m(\mathbf{s})| > L\varepsilon | \mathbf{s} \in \mathcal{S}\} \leq \delta_\varepsilon \\ & \Rightarrow \int_{\mathcal{S}} \mathbb{1}_{\{|h_p(\mathbf{u}) - h_m(\mathbf{u})| > L\varepsilon\}} d\mathbf{u} \leq \delta_\varepsilon \end{aligned} \quad (17)$$

Here, $\mathbb{1}$ is the indicator function (1 if $\{|h_p(\mathbf{u}) - h_m(\mathbf{u})| \geq L\varepsilon\}$ for $\mathbf{u} \in \mathcal{S}$). Let $\mathcal{S}^+ \subset \mathcal{S}$ such that $\forall \mathbf{s} \in \mathcal{S}^+$, $|h_p(\mathbf{s}) - h_m(\mathbf{s})| < L\varepsilon_m$ and $\mathcal{S}^- = \mathcal{S} \setminus \mathcal{S}^+$. Then (16) can be expressed as

$$\begin{aligned} B &\leq \int_{\mathcal{S}^+} |h_p(\mathbf{u}) - h_m(\mathbf{u})| \mathcal{P}(\mathbf{u}) d\mathbf{u} + \int_{\mathcal{S}^-} |h_p(\mathbf{u}) - h_m(\mathbf{u})| \mathcal{P}(\mathbf{u}) d\mathbf{u} \\ &\leq L\varepsilon_m \int_{\mathcal{S}^+} \mathcal{P}(\mathbf{u}) d\mathbf{u} + 2M \int_{\mathcal{S}^-} \mathcal{P}(\mathbf{u}) d\mathbf{u} \end{aligned} \quad (18)$$

$$\Rightarrow B \leq L\varepsilon_m + 2M\delta \text{ for any } \varepsilon_m > 0 \quad (19)$$

Here (18) follows from definition of \mathcal{S}^+ , L and M , and (19) follows from (17) and definition of $\mathcal{S}^+, \mathcal{S}^-$. Next, through direct application of Hoeffding’s inequality on C in (15), we get

$$C \equiv \mathbb{P}\left\{|\mathbb{E}[h_m(\mathbf{s})] - \widehat{\mathbb{E}}[h_m(\mathbf{s})]| \leq \varepsilon_h\right\} \geq 1 - \beta \quad (20)$$

where, $\varepsilon_h = \sqrt{\frac{4M^2 \log(2/\beta)}{N}}$ and N is the number of sample evaluations. Using (19) and (20) in (15) proves the theorem. \square

B. Proof of Theorem 2

Proof.

$$\begin{aligned} \mathbb{P}\{h_p(\mathbf{s}) > 0\} &\leq \mathbb{P}\{h_p(\mathbf{s}) > 0 \cap h_p(\mathbf{s}) > h_m(\mathbf{s})\} \\ &\quad + \mathbb{P}\{h_p(\mathbf{s}) > 0 \cap h_p(\mathbf{s}) \leq h_m(\mathbf{s})\} \\ &\leq \mathbb{P}\{h_p(\mathbf{s}) > h_m(\mathbf{s})\} \\ &\quad + \mathbb{P}\{h_p(\mathbf{s}) > 0 \cap h_p(\mathbf{s}) \leq h_m(\mathbf{s})\} \end{aligned}$$

as joint probability is always less than individual probabilities. $\mathbb{P}\{|V(\mathbf{s}^i) - \widehat{V}(\mathbf{s}^i)| > \varepsilon_m\} \leq \delta$. Here, by GP confidence bound $\mathbb{P}\{h_p(\mathbf{s}) - h_m(\mathbf{s}) > \varepsilon\} \leq \delta(\kappa)$ for any $\varepsilon \geq 0$, where κ decides the confidence level like $\kappa = 3$ for 99.7% success or $\delta(\kappa) = 0.003$. Thus,

$$\mathbb{P}\{h_p(\mathbf{s}) > 0\} \leq \delta(\kappa) + \mathbb{P}\{h_p(\mathbf{s}) > 0 \cap h_p(\mathbf{s}) \leq h_m(\mathbf{s})\}$$

Now breaking the joint probability as conditional probability $\mathbb{P}(A \cap B) = \mathbb{P}(A|B)\mathbb{P}(B)$

$$\leq \delta(\kappa) + \mathbb{P}\{h_p(\mathbf{s}) > 0 | h_p(\mathbf{s}) \leq h_m(\mathbf{s})\} \mathbb{P}\{h_p(\mathbf{s}) \leq h_m(\mathbf{s})\}$$

If $h_p(\mathbf{s}) \leq h_m(\mathbf{s})$ and $h_p(\mathbf{s}) > 0$ then $h_m(\mathbf{s}) > 0$. Thus,

$$\leq \delta(\kappa) + \mathbb{P}\{V_g^i > 0 | h_p(\mathbf{s}) \leq h_m(\mathbf{s})\} \mathbb{P}\{h_p(\mathbf{s}) \leq h_m(\mathbf{s})\}$$

Converting conditional into joint probability

$$\mathbb{P}\{h_p(\mathbf{s}) > 0\} \leq \delta(\kappa) + \mathbb{P}\{h_m(\mathbf{s}) > 0 \cap h_p(\mathbf{s}) \leq h_m(\mathbf{s})\}$$

Again, as joint probability is always less than individual probabilities

$$\mathbb{P}\{h_p(\mathbf{s}) > 0\} \leq \delta(\kappa) + \mathbb{P}\{h_m(\mathbf{s}) > 0\}$$

Applying Hoeffding’s inequality to GP-based probability estimation with $\varepsilon = \sqrt{\log(1/\beta)/2N}$

$$\mathbb{P}\left\{\mathbb{P}\{h_m(\mathbf{s}) > 0\} - \widehat{\mathbb{P}}\{h_m(\mathbf{s}) > 0\} \leq \varepsilon\right\} \geq 1 - e^{-2N\varepsilon^2}$$

$$\text{Or } \mathbb{P}\left\{\mathbb{P}\{h_m(\mathbf{s}) > 0\} \leq \varepsilon + \widehat{\mathbb{P}}\{h_m(\mathbf{s}) > 0\}\right\} \geq 1 - \beta$$

Thus,

$$\mathbb{P}\{h_p(\mathbf{s}) \geq 0\} \leq \delta(\kappa) + \varepsilon + \widehat{\mathbb{P}}\{h_m(\mathbf{s}) \geq 0\}$$

with confidence $1 - \beta$ \square